J Fluoresc (2013) 23:543–549
DOI 10.1007/s10895-013-1188-8

ORIGINAL PAPER

A Feasible Add-On Upgrade on a Commercial Two-Photon FLIM Microscope for Optimal FLIM-FRET Imaging of CFP-YFP Pairs

Lingling Xu · Liang Wang · Zhihong Zhang · Zhen-Li Huang

Received: 11 July 2012 / Accepted: 24 February 2013 / Published online: 3 March 2013

Abstract Fluorescence lifetime imaging microscopy (FLIM) based on time-correlated single photon counting (TCSPC) is a widely used method for fluorescence resonance energy transfer (FRET). Here we report a feasible add-on approach to upgrade a commercial two-photon FLIM microscope into a single-photon FLIM microscope which provides optimal FLIM-FRET imaging of FRET pairs consisting of cyan fluorescent proteins (CFPs) as the donor and yellow fluorescent proteins (YFPs) as the acceptor. The capability of the upgraded system is evaluated and discussed, and the imaging performance of the system is demonstrated using FLIM-FRET experiments with a representative CFP-YFP FRET pair (mCerulean-mCitrine).

Keywords Fluorescence resonance energy transfer (FRET) · Fluorescence lifetime imaging microscopy (FLIM) · Cyan fluorescent proteins (CFPs) · Yellow fluorescent proteins (YFPs)

Introduction

Forster resonance energy transfer (FRET) is a famous physical phenomenon which involves non-radiative energy transfer from excited fluorophore (called donor) to a nearby fluorophore (called acceptor) if this donor/acceptor pair (called FRET pair) is separated in a sufficient close distance (FRET distance, typically$<$10 nm) [1]. More importantly, the efficiency of this kind of energy transfer (FRET efficiency) depends on the FRET distance. Therefore, with the use of FRET pair labeled proteins, FRET microscopy offers unique opportunities for studying protein–protein interactions which are thought to play an important role in regulating many cellular signaling pathways [2].

In the past decades, various methods have been developed to quantify the FRET efficiency. Among them, fluorescence lifetime imaging microscopy (FLIM) is widely accepted to be the most rigorous method for determining the FRET efficiency, since FLIM-FRET method is based on the measurement of the of the fluorescence lifetime of the donor in the presence of FRET, which can be determined precisely without cross-talk artifacts [1, 2]. However, several limitations prevent the FLIM method from being the dominant approach for FRET imaging, while the most severe limitation comes from the specialized FLIM instrumentation which is expensive to obtain [2]. For example, as the most common implementation with laser scanning confocal microscopy (hereafter called confocal microscopy), time-domain FLIM requires at least two expensive components: time-correlated single-photon counting (TCSPC) module and laser with short pulse duration (typically tens of picoseconds or less) [1]. Therefore, attempts to extend the imaging capacity of existing FLIM-FRET system would be of great beneficial to expand the application fields of the FLIM-FRET method.

On the other hand, cyan fluorescent proteins (CFPs), such as Cerulean, are widely used as donor fluorophores in FRET microscopy when paired with yellow fluorescent proteins (YFPs) such as Citrine or Venus. And, great progresses have been made to develop better CFP variants

L. Xu · L. Wang · Z. Zhang · Z.-L. Huang
Britton Chance Center for Biomedical Photonics, Wuhan National Laboratory for Optoelectronics-Huazhong University of Science and Technology, Wuhan 430074, China

L. Xu · L. Wang · Z. Zhang · Z.-L. Huang (✉)
Key Laboratory of Biomedical Photonics of Ministry of Education, Department of Biomedical Engineering, Huazhong University of Science and Technology, Wuhan 430074, China
e-mail: leo@mail.hust.edu.cn

which show simultaneously large extinction coefficients, high quantum yields, and single exponential fluorescence lifetime [3]. Therefore, combining improved CFP-YFP pairs with FLIM method would be highly desirable for FRET experiments. However, as pointed out by Piston et al. [4], FLIM-FRET imaging of CFP-YFP pairs is not convenient since the optimized excitation wavelength (approximately 425 nm) is not found on most commercial confocal systems. For a technology replacement, Piston et al. suggested two-photon FLIM-FRET method which requires a tunable femtosecond Ti:Sapphire laser operating at 820 nm [4].

Unfortunately, although two-photon microscopy is superior for deep tissue (>100 μm) imaging, on thinner specimens the high light intensity within the focal volume (up to terawatts per square centimeter) can potentially induce undesirable destructive multi-photon effects [5]. In contrast to two-photon microscopy, conventional confocal microscopy typically employs a light intensity in the range of kilowatts per square centimeter. If the excitation wavelength in confocal microscopy is carefully chosen to be within the visible range, most photodestructive effects (in particular, UVA effects) can be avoided. Since the average size of suspended eukaryotic cells is <30 μm in diameter and would be even smaller when they are spread out on cover glasses [6, 7], it would be advantageous to use confocal microscopy to study dynamic protein interactions inside these living cells.

In this paper, we provided a feasible add-on approach to convert a commercial two-photon FLIM system into a single-photon FLIM-FRET system, while the functionality of the old system is still maintained. The FLIM-FRET imaging performance of the upgraded system was evaluated and discussed systematically.

Materials and Methods

Cell Culture

HeLa cells were cultured in Dulbecco's modified Eagle's medium (DMEM, Invitrogen) supplemented with 10 % fetal bovine serum (FBS) and maintained in humidified incubator at 37 °C with 5 % CO_2. The cells were seeded in 35-mm glass-bottomed dishes (LabTek) for confocal imaging 1 day before the transfection. Plasmids were transfected into Hela cells using Lipofectamine 2000 (Invitrogen) transfection reagent according to manufacturer's protocol. Plasmids for expressing mCerulean (mCer) alone, mCerulean-mCitrine pair seperated by a short (mCer-short-mCit, 12-amino-acid) or a long (mCer-long-mCit, 135-amino-acid) linker, and unlinked mCerulean and mCitrine (mCit) were used, respectively. Live cell imaging was performed 20 h after the transfection.

Fluorescence Lifetime Imaging Microscope

The microscope was upgraded from a commercial two-photon FLIM system and was shown in Fig. 1. The fundemental light from a tunable Ti:Sapphire laser (Mai Tai, Spectral-Physics; 100 fs pulse width, 80 MHz repetition rate) was focused by a double-convex lens (f=38.1 mm) into a second-harmonic generation (SHG) crystal (BBO, thickness=0.5 mm, Castech Inc, China). The frequency-doubled laser (SHG laser) after the BBO crystal was collimated and expanded with another double-convex lens (f=100 mm), cleaned by an infrared cut-off filter (BG39), and sent to an Olympus FV1000 scan head via the dichroic mirror which was previously designed for coupling a 405 nm LD laser (DM2, after shifting the fiber connector to a farer position). The SHG laser was reflected by DM3 which was designed for coupling infrared laser for two-photon excitation, reflected again by DM4 which was designed for separating excitation laser and fluorescence emission (see Results and Discussions for further information), and focused into biological samples by an Olympus 60x/NA1.42 oil immersion objective lens equipped in an Olympus IX 81 inverted microscope. Note that the beam diameter of the SHG laser was expanded to fill the back aperture of the objective lens through the combination of the two double-convex lenses. With tuning the Ti:Sapphire laser from 780 nm to 870 nm, one-photon excitation from 390 nm to 435 nm (limited by the transmission curve of DM2) can be obtained from this configuration.

Fluorescence signal was collected by the same objective len, guided back to the FV1000 scan head, passed through DM4, coupled into a multi-mode fiber (UV 800/880, A. R. T. Photonics GmbH, Core diameter=800 μm, Length=1 m) via a confocal detection port in the FV1000 scan head, and spreaded into 16 spectral channels via the polychromator inside a PML-Spec multi-spectral detection system (Becker & Hickl). To minimize scattered laser, a bandpass filter (FF01-554/211-25, Semrock) was placed between the multi-mode fiber and the PML-Spec. The electronic signal generated from the PML-Spec detection system was sent to a SPC-830 TCSPC module (Becker & Hickl) for further analysis. The SPCM software provided by Becker & Hickl was used to allow fluorescence lifetime imaging during the scanning process. Lifetime decay curves were analyzed with the SPCImage (Becker & Hickl).

Data Analysis

The FRET efficiency (E) can be measured by the following well-known equation consisting of the lifetime values of the interacting (τ_{FRET}) and noninteracting donor (τ_D) [8].

$$E = 1 - \frac{\tau_{FRET}}{\tau_D} \quad (1)$$

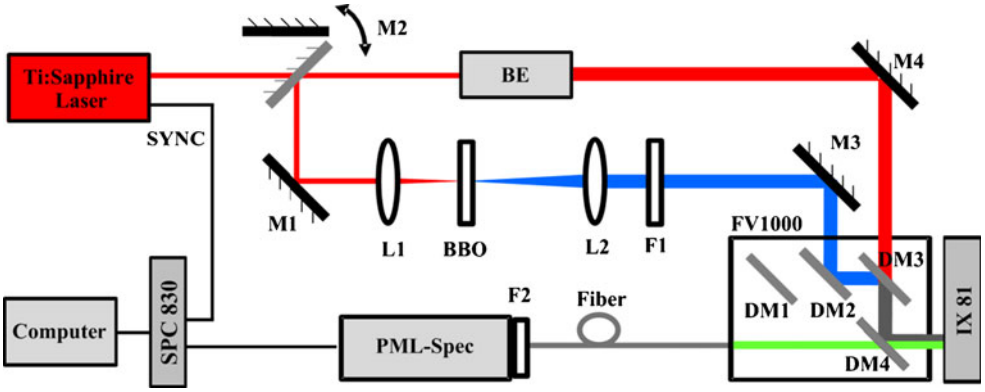

Fig. 1 Illustration of the single-photon TCSPC FLIM system. L: Lens; Lens1: focal length= 38.1 mm, diameter=25.4 mm; Lens2: focal length=100 mm, diameter=25.4 mm; M: mirror; F: filter; BE: beam expander; BBO: second-harmonic generation (SHG) crystal; DM: dichroic mirror; SYNC: synchronization signal from Ti: Sapphire laser

The standard deviation of E (σ_E) can be obtained using error propagation formula [9].

$$\left(\frac{\sigma_E}{E}\right)^2 = \left(\frac{\sigma_{\tau_{FRET}}}{\tau_{FRET}}\right)^2 + \left(\frac{\sigma_{\tau_D}}{\tau_D}\right)^2 \quad (2)$$

Results and Discussion

Optimizing the Excitation and Emission Wavelengths for CFP-YFP FRET Pair

To maximize FRET measurement accuracy, it is of great beneficial to optimize the excitation wavelength. Previously, Piston et al. [4] employed a complicated method, which is based on the measurement of five different excitation or emission spectra, and calculated that the optimal excitation wavelength is ~427 nm for the mCer-mCit pair. In this study, we are interested to develop a much simpler method which presents similar results as that from Piston et al.

We notice that, basically, the optimized excitation locates at the wavelength that maximizes donor excitation and minimizes direct excitation of the acceptor. In other words, the optimized wavelength for the mCer-mCit FRET pair should be located at the peak of the normalized donor (mCer) excitation spectra ($Ex_{mCer}^{normalized}(\lambda)$) divided by the normalized acceptor excitation spectra ($Ex_{mCit}^{normalized}(\lambda)$). Therefore, since the crossover point between $Ex_{mCer}^{normalized}(\lambda)$ and $Ex_{mCit}^{normalized}(\lambda)$ is located at 475 nm (see Fig. 2a), the optimal excitation wavelength should be at a wavelength lower than 475 nm. The exact value for this optimal wavelength can be easily obtained by plotting the ratio of $Ex_{mCer}^{normalized}(\lambda)$ to $Ex_{mCit}^{normalized}(\lambda)$ as a function of wavelength (Fig. 2b), which has a peak at ~427 nm. In comparison with the wavelength obtained by Piston et al., our method presents almost the same value while is surprisingly simple.

It is also important to determine a suitable emission wavelength range which maximizes the detection of donor fluorescence and minimizes the detection of acceptor fluorescence. In a similar way to the determination of optimal excitation wavelength, the optimal emission wavelength range can be obtained by finding the cutoff wavelength from the normalized donor (mCer) emission spectra ($Em_{mCer}^{normalized}(\lambda)$) divided by the normalized acceptor emission spectra ($Em_{mCit}^{normalized}(\lambda)$). Therefore, it can be easily estimated from Fig. 2a that the detection wavelength should locate at<525 nm (the crossover point between $Em_{mCer}^{normalized}(\lambda)$ and $Em_{mCit}^{normalized}(\lambda)$). A further

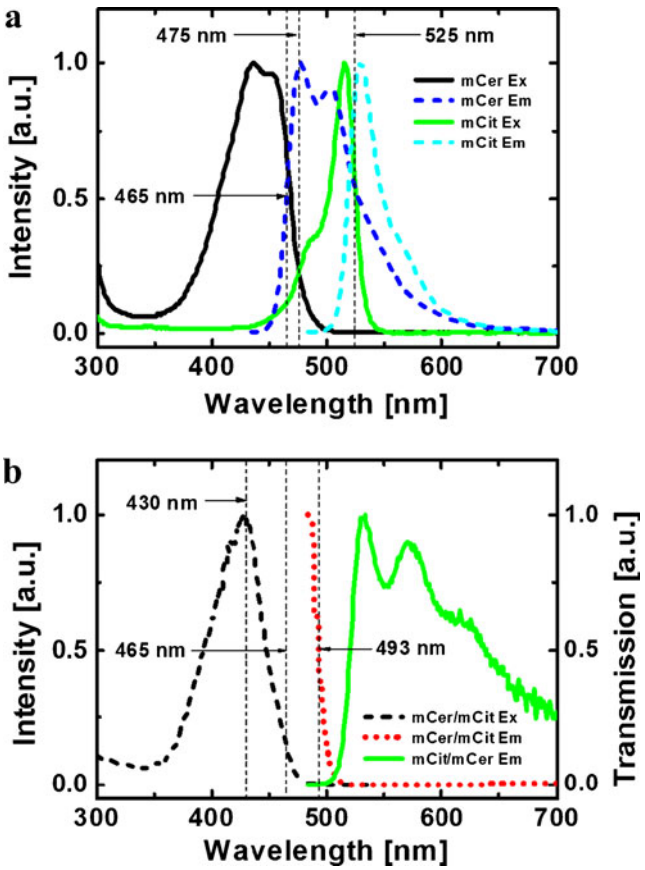

Fig. 2 **a** The excitation and emission spectra of the proteins alone (from Roger Tsien's Lab). **b** Optimized excitation and emission wavelengths for the mCer-mCit FRET pair, and the transmission curve of the most suitable DM4

calculation of the ratio of $Em_{mCer}^{normalized}(\lambda)$ to $Em_{mCit}^{normalized}(\lambda)$ confirmed that the detection wavelength should be< 493 nm. Here we recommend the red cutoff wavelength with a ratio>0.5 ($Em_{mCer}^{normalized}(\lambda)/Em_{mCit}^{normalized}(\lambda)$) to guarantee sufficient high fluorescence contribution from the donor. On the other hand, the blue cutoff wavelength can be estimated where the intensity is 50 % of the emission peak. For the mCer-mCit FRET pair, the blue cutoff wavelength was calculated to be ~465 nm (see Fig. 2a). Therefore, the optimal emission wavelength range for the mCer-mCit FRET pair is 465–493 nm.

Converting a Two-Photon FLIM into a Single-Photon FLIM System

Considering that a pulse laser (hundreds of picoseconds or shorter [10]) is necessary for TCSPC FLIM imaging and the optimal excitation wavelength for the mCer-mCit FRET pair is 427 nm, the fundemental laser from the tunable Ti: Sapphire laser (which is already available in the commercial two-photon microscopy) was frequancy-doubled by a famous second-harmonic generation crystal BBO (see details in the Materials and Methods section and following sections). In this case, we avoided the purchase of new expensive pulse lasers, though an additional electronic delay cable may be required to compensate the optical path difference between the two-photon and single-photon FLIM systems.

Then, it is necessary to consider how to introduce the SHG laser into the FV1000 system which has three laser ports: DM1 for VIS lasers (including 458–515 nm Argon ion laser, green (543 nm) and red (633 nm) HeNe lasers), DM2 for UV laser (405 nm laser diode) and DM3 for NIR laser (~700–1000 nm from the Ti:Sapphire laser). Taking the optimal excitation wavelength for the mCer-mCit FRET pair into consideration, DM2 was chosen to import the SHG laser. To maintain the function of the original FLIM system, the fiber connector for the LD405 laser was adjusted slightly far away from the FV1000 scan head, and a flip mirror was placed before DM2 and the LD405 fiber connector to switch between LD405 and the SHG laser.

Inside the scan head of commercial FV1000 system, four dichroic mirrors (DM4) are available for reflecting LD405 laser and passing through fluorescence emission. We measured the transmission curves of these dichroic mirrors (Fig. 3) and found that DM 458/515 is suitable for FLIM-FRET imaging of the mCer-mCit pair which requires an optimal excitation wavelength of 427 nm and an emission wavelength range of 465–493 nm.

For our fluorescence detection system, the detection wavelength of the multi-spectral detector (PML-Spec) covers from 300 nm to 800 nm through adjusting the angle of the grating inside, while at each grating position fluorescence signal with

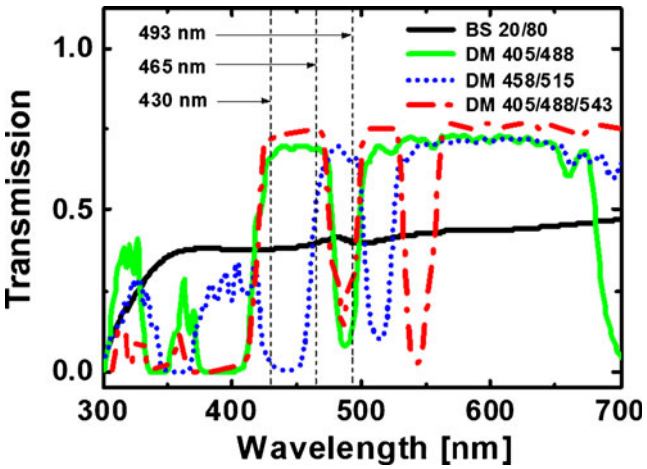

Fig. 3 Transmission curves of DM4 sets

a bandwidth of ~200 nm spreads successively into 16 separated spectra channels. Taking the optimal excitation and emission wavelengths for the mCer-mCit FRET pair (see above) and the FLIM detector parameters into consideration, the FLIM-FRET measurement is performed at the wavelength range of 470–495 nm in this study.

It is worthy to note that the system conversion shown above is not only suitable for the Olympus FV1000. For other commercial two-photon microscope systems which also consist of ports for coupling UV and visible lasers, system upgrade can be performed with similar procedures.

Characterizing the Available Laser Power in the Single-Photon FLIM System

It would be necessary to evaluate whether the available SHG laser power is sufficient for single-photon FLIM imaging. Notice that the maximum available SHG laser power after passing through a microscope objective ($P_{SHG}^{\max}$) is the product of the maximum laser power of fundamental near-infrared femtosecond laser ($P_{NIR}^{\max}$), the frequency doubling efficiency (Φ_{SHG}) and the transmission efficiency of the optical system (T_{system}), that is, $P_{SHG}^{\max} = P_{NIR}^{\max} * \Phi_{SHG} * T_{system}$. For our femtosecond laser, $P_{NIR}^{\max}$ is up to 1.5 W. Maximum Φ_{SHG} was obtained (Fig. 4a) by adjusting the level angle and pitch angle of the BBO crystal. We found that for a SHG laser at ~430 nm (which is close to the optimal excitation wavelength of the mCer-mCit FRET pair), the maximum P_{SHG} is 130 mW (Fig. 4b) and the maximum T_{system} is 7.26 % (Fig. 4c).

It should be noted that the transmission efficiency of the optical system depends not only on the transmission curves of DM4 (Fig. 3), but also other optical elements inside the optical path (especially DM2 which designed to reflect only UV laser, Fig. 1). In fact, we found that the transmission efficiency of the optical system drops rapidly at wavelength

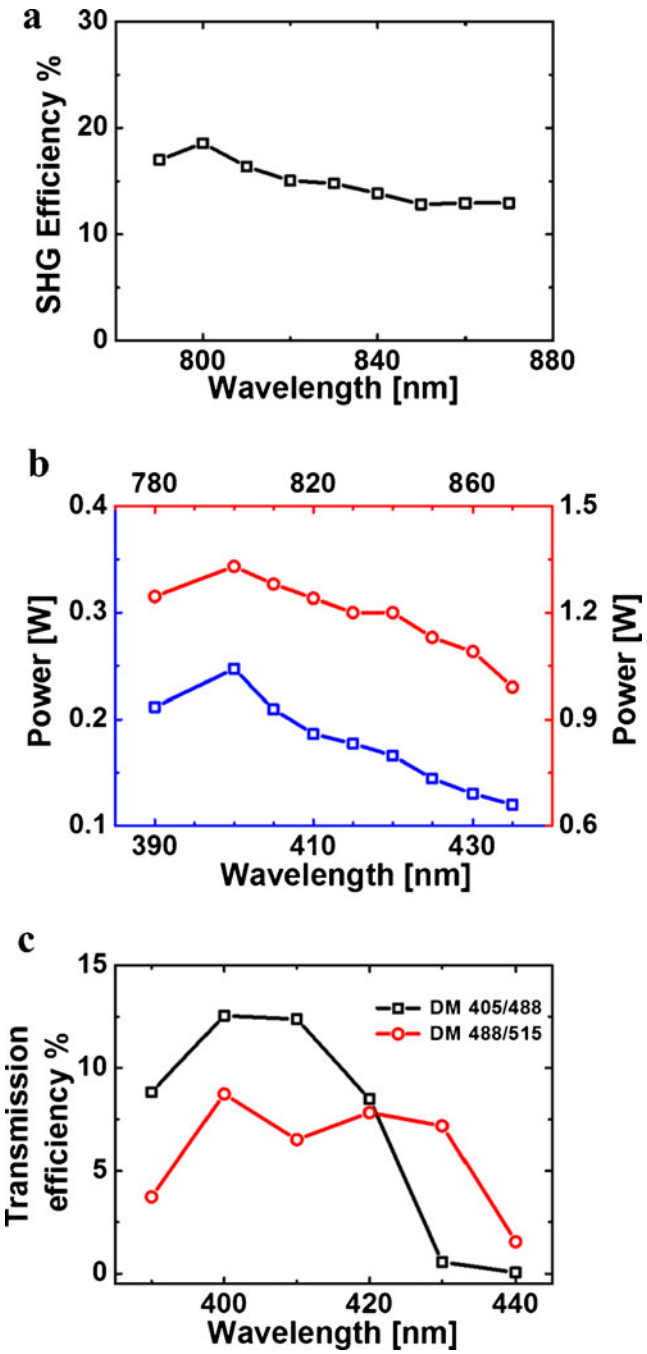

Fig. 4 The SHG efficiency (**a**), maximum SHG laser power (**b**), and transmission efficiency of the optical system (**c**). The SHG efficiency is the ratio of SHG laser power (*blue rectangulars* in **b**) and fundamental laser power (*red circles* in **b**). The transmission efficiency of the optical system is the laser power after passing the Olympus 60x/NA1.42 objective divided by the SHG laser power before entering the FV1000 scan head. Note that the transmission efficiency of the optical system depends on different DM4

longer than 420 nm when DM 405/488 was used as DM4. Therefore, for FLIM-FRET imaging of the mCer-mCit FRET pair, it is better to use DM 458/515 as DM4, which provides higher transmission efficiency for 430 nm laser (Fig. 4c) and 465–495 nm fluorescence emission (Fig. 3). For FLIM imaging using wavelength>435 nm, it may be necessary to use the other laser port (DM1) to couple the SHG laser into the FV1000 scan head. Nevertheless, in the current configuration of our single-photon FLIM system, the excitation laser is available in the wavelength range from 390 to 435 nm. And confocal imaging is usually performed using<5 % of the available SHG laser. Note that this SHG wavelength range is currently limited to the available fundamental laser output from our femtosecond Ti: Sapphire laser. A much broader range (350–500 nm) is possible with the combination use of a properly working femtosecond laser and a suitable laser port (for coupling the SHG laser).

Characterizing the Imaging Performance of the Single-Photon FLIM System

The imaging performance of a single-photon TCSPC FLIM system not only depends on the available laser wavelength and power, but also on field illumination evenness and Instrumental Response Function (IRF). After centering the SHG laser spot to the center of the illumination field [11], we characterized the field illumination evenness of the single-photon FLIM system and found that the intensity at the far end of the fluorescence image drops to~75 % of the peak intensity in the center (Fig. 5).

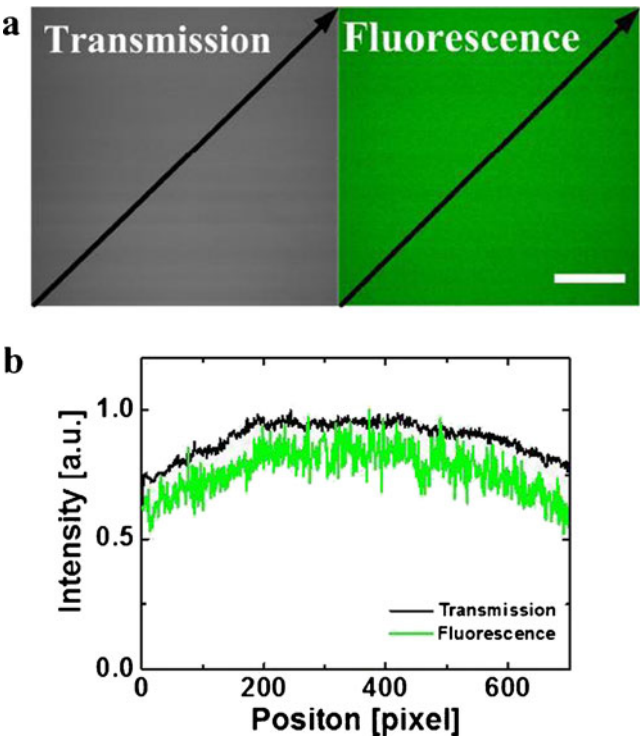

Fig. 5 Characterizing field illumination evenness. **a** Transmission image (*left*) and fluorescence image (*right*) of dilute fluorescein in water. **b** The line profiles of the area indicated by the *black arrows* in (**a**). *Scale bar*: 50 μm

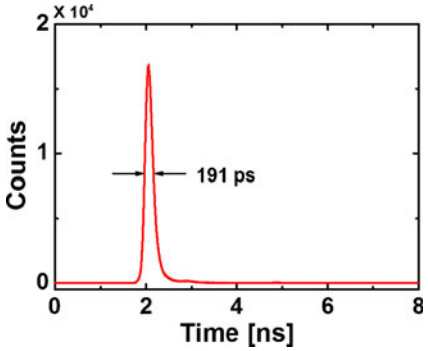

Fig. 6 IRF measurement of our single-photon FLIM system. The excitation laser was 430 nm

We also characterized the IRF of the single-photon FLIM system by replacing the fluorescein solution with a cover slice which reflects a small amount of 430 nm laser to the detection system. The IRF was found to have the full width at half-maximum (FWHM) of 191 ps (Fig. 6), which is close to the reported value in the literature (150–200 ps) [12]. Finally, we note that it is better to leave enough time channels before the rising of the IRF signal (1.5~2 ns in our FLIM setup), so that lifetime measurements can be performed more accurately. If the rising of the IRF signal locates before 1 ns, it is hard to obtain accurate lifetime values in FLIM experiments.

To verify the accuracy of our single-photon FLIM system, we measured the lifetime of Rhodamine B in water as the standard sample at room temperature (25 °C). In our result, the lifetime of Rhodamine B is 1.53 ns (Fig. 7), which is close to the reported values [13]. This demonstrates that we can obtain the accuracy lifetime using our single-photon FLIM system.

Imaging mCerulean-mCitrine FRET Pair with the Single-Photon FLIM System

To demonstrate the imaging capability of our single-photon FLIM system, we performed FLIM-FRET experiments in

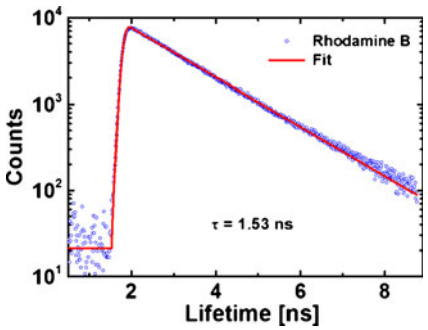

Fig. 7 Verifying performance of FLIM using Rhodamine B in water. Excitation wavelength was 430 nm, and emission band was 470–670 nm. The measure lifetime data of Rhodamine B (*blue circles*) were fit (*red line*) using single exponential model

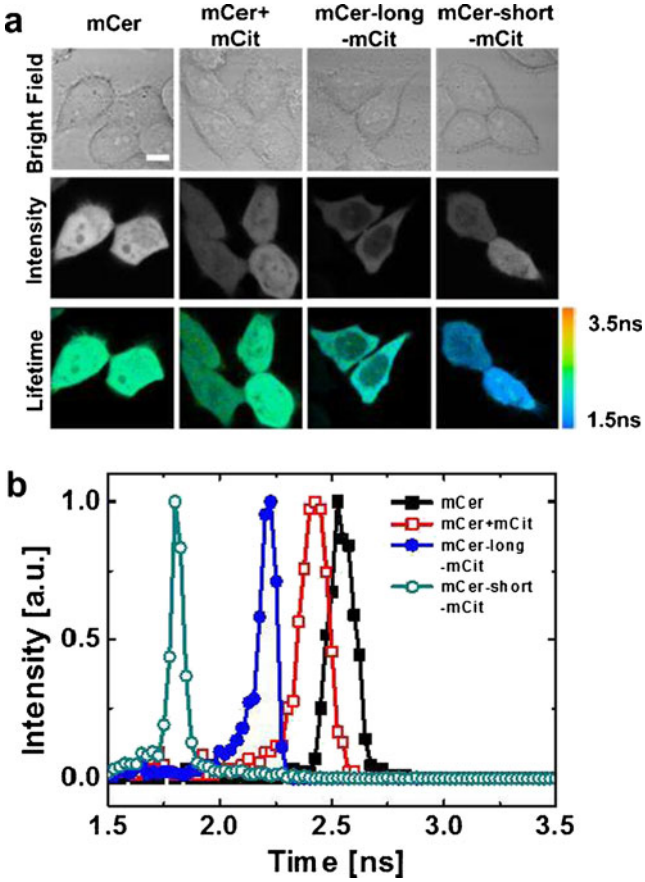

Fig. 8 FLIM-FRET imaging of HeLa cells expressing mCerulean and mCitrine. **a** Bright field, intensity and lifetime images. **b** Fluorescence lifetime distribution curves. *Scale bar*: 50 μm

HeLa cells expressing mCer, mCerulean-short-mCitrine (with 12 amino acids), mCerulean-long-mCitrine (with 135 amino acids), and coexpressing mCerulean and mCitrine (mCer+mCit). The excitation wavelength was 430 nm, and the fluorescence emission was detected in a wavelength range between 470 nm and 495 nm. Results are shown in Fig. 8. The measured mean fluorescence lifetime of mCer is close to the reported values [4, 14].

Fluorescence lifetime distribution curves clearly show that mCer alone has the longest lifetime, while the mCer-mCit pair separated by a short linker exhibits the shortest

Table 1 Average fluorescence lifetime and FRET efficiency

Sample	Mean±SD (ns)	E±SD
mCer	2.48±0.03	—
mCer+mCit	2.40±0.02	0.03±0.02
mCer-long-mCit	2.27±0.05	0.08±0.03
mCer-short-mCit	1.85±0.03	0.25±0.02

E: FRET efficiency. SD: standard deviation. Values were from at least 10 cells

lifetime. Using the data analysis procedure described in the Materials and Methods section, FRET efficiency in the four samples can be obtained from the lifetime values (Table 1). The FRET efficiencies observed for the mCer-mCit pair were consistent with linker length, with shorter linkers generating higher FRET efficiencies [4]. And it was consistent with the result using the acceptor photobleaching method (data not shown). These findings clearly verified the FLIM-FRET imaging capability of our single-photon FLIM system.

Conclusion

In this paper, we reported a feasible approach to upgrade a commercial two-photon FLIM system into a single-photon FLIM system. Through FLIM-FRET imaging in HeLa cells expressing mCerulean and mCitrine, we verified that the upgraded system is capable of performing single-photon FLIM-FRET imaging for popular CFP-YFP FRET pairs. We also provided a simple method to determine the optimal excitation and emission wavelengths for the mCer-mCit FRET pair. Comparing to the reported method, our method presents almost the same value while is surprisingly simple.

Acknowledgments This work was supported by National Basic Research Program of China (Grant No. 2011CB910401), the Science Fund for Creative Research Group of China (Grant No. 61121004), the National Natural Science Foundation of China (Grant No. 30970691), the Program for New Century Excellent Talents in University of China (Grant No. NCET-10-0407), and the Fundamental Research Funds for the Central Universities (Grant No. 2011TS087). We thank professor Fu-Jen Kao from National Yang-Ming University for helpful discussions, Dr. David Piston for providing pmCerulean-C1, Dr. Joel Swanson for providing pmCitrine-C1, and Dr. Jun Chu for proving mCerulean –short-mCitrine and mCerulean-long-mCitrine.

References

1. Pietraszewska-Bogiel A, Gadella TWJ (2011) FRET microscopy: from principle to routine technology in cell biology. J Microsc 241(2):111–118. doi:10.1111/j.1365-2818.2010.03437.x
2. Piston DW, Kremers GJ (2007) Fluorescent protein FRET: the good, the bad and the ugly. Trends Biochem Sci 32(9):407–414. doi:10.1016/j.tibs.2007.08.003
3. Markwardt ML, Kremers GJ, Kraft CA, Ray K, Cranfill PJC, Wilson KA, Day RN, Wachter RM, Davidson MW, Rizzo MA (2011) An improved Cerulean fluorescent protein with enhanced brightness and reduced reversible photoswitching. PLoS One 6(3). doi:10.1371/journal.pone.0017896
4. Rizzo MA, Springer G, Segawa K, Zipfel WR, Piston DW (2006) Optimization of pairings and detection conditions for measurement of FRET between cyan and yellow fluorescent proteins. Microsc Microanal 12(3):238–254. doi:10.1017/s1431927606060235
5. Pawley JB (2006) Handbook of biological microscopy, 3rd edn. Springer, New York
6. Fiolka R, Belyaev Y, Ewers H, Stemmer A (2008) Even illumination in total internal reflection fluorescence microscopy using laser light. Microsc Res Tech 71(1):45–50. doi:10.1002/jemt.20527
7. Karp G (2010) Cell and molecular biology: concepts and experiments, 6th edn. John Wiley & Sons Inc., New York
8. Berezin MY, Achilefu S (2010) Fluorescence lifetime measurements and biological imaging. Chem Rev 110(5):2641–2684. doi:10.1021/cr900343z
9. Fornasini P (2008) The uncertainty in physical measurements: an introduction to data analysis in the physics laboratory. Springer, New York
10. Becker W (2005) Advanced time-correlated single photon counting techniques, 1st edn. Springer, Berlin
11. Zucker RM (2006) Quality assessment of confocal microscopy slide based systems: performance. Cytometry A 69A(7):659–676. doi:10.1002/cyto.a.20314
12. Becker W (2010) The bh TCSPC Handbook, 4th edn. Becker & Hickl GmbH, Berlin
13. Muller CB, Weiss K, Loman A, Enderlein J, Richtering W (2009) Remote temperature measurements in femto-liter volumes using dual-focus-Fluorescence Correlation Spectroscopy. Lab Chip 9(9):1248–1253. doi:10.1039/b807910b
14. Rickman C, Duncan RR (2010) Munc18/Syntaxin interaction kinetics control secretory vesicle dynamics. J Biol Chem 285(6):3965–3972. doi:10.1074/jbc.M109.040402